

A Unified Approach to Kinship Verification

Eran Dahan and Yosi Keller



Abstract—In this work, we propose a deep learning-based approach for kin verification using a unified multi-task learning scheme where all kinship classes are jointly learned. This allows us to better utilize small training sets that are typical of kin verification. We introduce a novel approach for fusing the embeddings of kin images, to avoid overfitting, which is a common issue in training such networks. An adaptive sampling scheme is derived for the training set images to resolve the inherent imbalance in kin verification datasets. A thorough ablation study exemplifies the effectivity of our approach, which is experimentally shown to outperform contemporary state-of-the-art kin verification results when applied to the Families In the Wild, FG2018, and FG2020 datasets.

Index Terms—Kinship Verification, Face Recognition, Face Biometrics, Convolutional Neural Networks, Multi-Task Learning.

1 INTRODUCTION

The goal of kin verification [1], [2], [3], [4] is to verify whether or not two people are related by a particular kin relationship given their face images. The kinship classes are depicted in Fig. 1, where given a pair of face images $\{\phi_i, \varphi_i\}$ and a kinship class $\lambda_i \in \Lambda = \{\text{B-B, F-S, M-D, S-S, F-D, M-S, SIBS}\}$, we aim to verify whether ϕ_i and φ_i are related by λ_i . In contrast to face recognition, kin faces are non-identical, and their visual similarity is often unintuitive, even for human observers, as kins might differ by gender and notable age differences. The facial similarity of kins varies significantly between different families and even within the kins of a particular family, implying significant intraclass variability. As face recognition schemes aim to identify individual subjects, kins will be identified as different individuals. Following the common approach in face recognition, classical kin verification schemes encoded the input faces $\{\phi_i, \varphi_i\}$ using handcrafted features $\{\hat{\phi}_i, \hat{\varphi}_i\}$ [5], [6], [7] such as LBP, HOG, and Gabor. The representation was refined using metric-learning [8], [9], [10], and the kinship was classified by applying KNN and SVM classifiers. With the emergence of deep learning, it was applied to kin verification. Facial features were derived by training face recognition CNNs on large-scale face recognition datasets [11] and using transfer learning to apply them to kin verification [11]. Recent results by Wang et al. [12] applied a Generative Adversarial Net (GAN) to mitigate the age-differences by synthesizing face images depicting intermediate ages. Small-scale datasets were initially utilized in kin

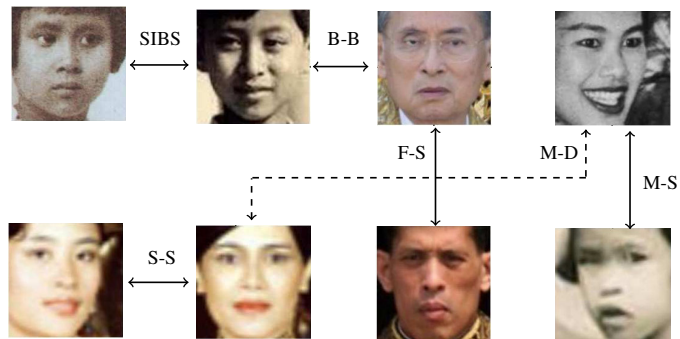


Fig. 1. The kinship verification task is to determine whether two face images are related by a particular kinship class, such as Brothers (B-B), Sisters (S-S), Father-Daughter (F-D), Father-Son (F-S), Mother-Son (M-S), Mother-Daughter (M-D), and Siblings (SIBS).

verification [5], [13], [14], most of which were shown [15], [16] to be biased, as the faces of kins were often cropped from the same photo, implying that the kinship could be inferred from the similar chromatic properties of the photo crops. The large-scale RFIW dataset [17] was the only one shown to be unbiased, consisting of kin pairs cropped from different photos. The novel FIW in Multimedia (FIW-MM) database, recently introduced by Robinson et al. [18], is a large-scale multi-modal kin verification dataset, consisting of video, audio, and contextual transcripts

In this work, we propose a deep learning-based approach for kin verification using a siamese CNN. We apply multi-task learning to train a single unified CNN for *all* kinship classes, allowing to leverage their training samples to refine the face embedding backbone CNN. We show that kin verification, in contrast to face recognition, is prone to overfitting and derive a novel CNN architecture for the fusion of face embeddings based on transposed 1×1 convolutions. We also show that kin verification datasets are inherently imbalanced in terms of the number of samples per family, and samples per kin (father, mother, etc.), implying that the training process might be biased. For that, we propose an adaptive sampling scheme for the training set, which is shown to improve the kin verification accuracy. Some kin verification classes, such as B-B and D-D, are symmetrical, allowing to utilize siamese CNNs. In contrast, other kinship classes, such as F-D, F-S, etc., are asymmetric in terms of age and gender, requiring different CNNs for each class. For that, we applied an asymmetric weighting layer that improves accuracy.

• E. Dahan & Y. Keller are with the Faculty of Engineering, Bar-Ilan University, E-mail:yosi.keller@gmail.com

In particular, we propose the following contributions: (1) We present a unified approach for kin verification that applies multi-task learning to jointly utilize the training sets of all kinship classes. (2) We show that kin verification is prone to overfitting and suggest a novel subnetwork for the fusion of feature maps based on cascaded 1×1 convolutions. (3) To overcome the imbalanced training set, we introduce an adaptive approach for sampling the training pairs, that is shown to improve the kin verification accuracy. (4) The proposed scheme is experimentally shown to outperform contemporary state-of-the-art approaches, when applied to the RFIW [17], FG2018, and FG2020 [19] datasets.

2 RELATED WORK

Kin verification is related to face verification, and similar approaches were often used [17]. Thus, early kin verification schemes utilized handcrafted image descriptors for encoding the face images. Puthenpuhussery et al. [6] used SIFT descriptors and genetic fisher vectors to optimize the similarity between true and false kins. Similarly, Fang et al. [5] applied LBP, HOG, and Gabor descriptors to encode the face images and trained KNN and Kernel SVM classifiers. LBP was used as a local face descriptor by Dander and Limbate, [7]. The informative patches in the face images were detected by Quin et al. [20] by applying sparse regularized group lasso regression to a SIFT-based face descriptor. The resulting face embeddings were classified by a linear SVM.

Mahpod and Keller [21], [22] proposed a metric-learning-based approach, applying symmetric and asymmetric metric learning to face embeddings using handcrafted features. The resulting representations were classified by an SVM classifier, and the scheme was applied to the KinFaceW-I and KinFaceW-II datasets [14]. A color histogram was found to be the most informative image feature, corresponding to the later findings by Lopez et al. [15] and Damson *et al.* [16] who showed these datasets, among others, to be color-biased. A neighborhood repulsed correlation-metric-learning approach was used by Yang [10], while Xn and Shan proposed an ensemble of bilinear models [23], where each model was trained by metric-learning using multiple face descriptors. Handcrafted image descriptors, such as LBP and Fisher vectors, were used in the Triangular Similarity Metric-Learning (TSML) approach by Pilei et al. [8], where the dimensions of the descriptors were reduced by metric learning. Optimal weights per feature were computed by Hairpin et al. [9] in the Discriminative Multimetric-Learning (DML) scheme, and the weighted features were used within a metric learning formulation.

With the emergence of deep learning, CNNs were also applied to kin verification. Lu et al. [24], proposed discriminative deep metric-learning (DML) to train a CNN to jointly learn multiple metric-learning networks, and use ensemble-learning to optimize the results. An asymmetric scheme, where each image is processed by a different CNN that is adjusted to the input (Father, Son, etc.), was proposed by Avignon et al. [25], where metric-learning was applied to the face embeddings. A coarse-to-fine domain adaptation approach was derived by Duad et al. [11] to utilize the deep features learned by a face recognition network as kin verification features.

A large-scale kin verification evaluation by human reviewers was conducted by Kohl et al. [26], who proposed a hierarchical verification scheme, using representation learning to encode the face regions. The Kinnet CNN was introduced by Li et al. [27], where the face embeddings were learned using a large-scale face recognition dataset. A triplet loss was applied to learn the kin verification, and the number of images per family member was balanced by image augmentation. An ensemble of four CNNs was applied to improve the accuracy. Kohl et al. [28] applied autoencoders to detect kin similarity in unconstrained videos, using a supervised mixed-norm autoencoder to compute the sparse embeddings of the kin pairs. Deep autoencoders were also studied by Deadman et al. [29] to detect informative facial features for kin verification, where a Sparse Discriminative Metric Loss (SDM-Loss) was derived to utilize the positive and negative training pairs. A review and evaluation of contemporary schemes were detailed in the RFIW 2020 challenge [19], organized by Robinson et al.

A Generative Adversarial Net (GAN) was proposed by Wang et al. [12] to mitigate the age differences by synthesizing younger and older face images of parents and their siblings, respectively. Thus, a conditional GAN was used to synthesize cross-generation kins in an intermediate age domain, to improve the face similarity. Ozkan and Ozkan [30] proposed a GAN-based approach for synthesizing an image of a child’s face using the face images of a single parent. The synthesis is derived by a generator network in an auto-encoder architecture. An adversarial loss was applied using large-scale unsupervised data, to mitigate the overfitting, due to the small annotated training sets. The stability of the approach was improved using cycle-consistency. Gao et al. [31] introduced a novel biologically-motivated kinship generation approach, where the facial appearance of a child is inherited from both parents by a random genomic fusion process. For that, a three-step approach was derived, where first a conditional auto-encoder (CAD) is trained on a large-scale face dataset to encode the facial appearance given age and gender. Second, a CNN denoted as DNA-Net is trained to further encode the face embeddings into an embedding denoted as genes. Random subsets of male and female genes are combined and decoded by the CAD decoder to synthesize the child’s face.

A fundamental flaw in most contemporary kin and family verification image datasets was detected by Lopez et al. [15], who noticed that the KinFaceW datasets were created by cropping the kin face images from the same family photographs. Hence, learning-based schemes in general, deep learning-based in particular, might learn the chromatic (“from same photo”) cues instead of the kinship similarity. Dawson et al. [16] extended these results by training the deep learning-based From Same Photo (FSP) image classifier that was trained to detect whether two image patches were cropped from the same photo. The FSP was applied to most contemporary kin face datasets, achieving accurate kinship classification in all, but for the RFIW dataset. Thus, in this work, we evaluate the proposed scheme by training it, using only the RFIW dataset [17]. A thorough survey by Robinson et al. [32] details recent approaches and datasets in kin verification.

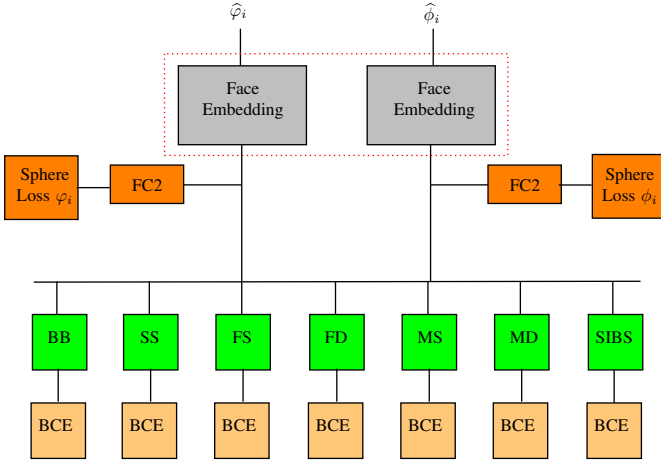


Fig. 2. The proposed kin verification system. The logical components are color-coded. The face embedding CNN is shared by all kinship classes and is initially pretrained on the CASIA-WebFace face image dataset [33]. The embeddings $\hat{\varphi}_i$ and $\hat{\phi}_i$ of the input face images are fused and classified by separate subnetworks, one per kinship class. The weight-sharing FC-2 layer is used to refine the face embedding on the RFIW dataset [17].

3 UNIFIED MULTI-TASK KIN VERIFICATION

In this work, we propose a unified multi-task kin verification approach, where all kinship classes are jointly learned, using the CNN depicted in Fig. 2. It consists of a siamese network for learning the face embeddings used in the classification of all of the kinship classes, followed by multiple kinship classification subnetworks, one per kin verification task, e.g., B-B, SIBS.

The embeddings $\{\hat{\varphi}_i, \hat{\phi}_i\}$ of $\{\phi_i, \varphi_i\}$ are computed using the siamese CNN detailed in Section 3.1. $\{\hat{\varphi}_i, \hat{\phi}_i\}$ are jointly trained end-to-end using *all* kinship classes and corresponding images in the training set. In contrast, in previous schemes [17], a separate classification CNN was trained per kinship class, utilizing an order of magnitude less training images. Each kin verification triplet $\{\hat{\varphi}_i, \hat{\phi}_i, \lambda_i\}$ is classified by the embedding-fusion and classification subnetwork depicted in Fig. 2. There are $|\Lambda| = 7$ such subnetworks that are detailed in Section 3.2. A novel embedding-fusion approach is introduced in Section 3.2, based on channel-wise 1×1 convolutions, to avoid overfitting. The overfitting issue was previously reported by Robinson et al. [17] when applying distance learning to face embeddings computed using the Sphreface CNN, resulting in little classification accuracy improvement. Kin verification datasets in general, and the RFIW dataset [17] in particular, are inherently imbalanced, with respect to the number of images per family, and the number of images per kin, in each family. For that, we propose in Section 3.3 an adaptive image sampling scheme that is shown to improve the verification accuracy.

The proposed scheme is trained using multiple losses. The siamese face embedding CNN is refined using the Sphere losses $L_{Sphere}^{\hat{\varphi}_i}$ and $L_{Sphere}^{\hat{\phi}_i}$, that are applied to classify the embeddings $\{\hat{\varphi}_i, \hat{\phi}_i\}$ of the 10,676 identities in the RFIW dataset. The kin verification is classified using the $|\Lambda| = 7$ subnetworks trained using $\{L_{BCE}^{\lambda_i}\}_{\lambda_i \in \Lambda}$ Binary

Cross-Entropy (BCE) losses, such that $L_{BCE}^{\lambda_i}$ verifies the kinship λ_i . Given a particular training triplet $\{\hat{\varphi}_i, \hat{\phi}_i, \lambda_i\}$, all other BCE losses are zeroed

$$\{L_{BCE}^{\lambda_k}\} = 0, \forall \lambda_k \in \Lambda, \lambda_k \neq \lambda_i. \quad (1)$$

Thus, the overall loss is given by

$$L(\hat{\varphi}_i, \hat{\phi}_i, \lambda_i) = L_{Sphere}^{\hat{\varphi}_i} + L_{Sphere}^{\hat{\phi}_i} + \alpha^2 \sum_{\lambda_k} L_{BCE}^{\lambda_k} \cdot \Delta(\lambda_k - \lambda_i) \quad (2)$$

where

$$\Delta(x) = \begin{cases} 1, & x = 0 \\ 0, & \text{else} \end{cases}, x \in \mathbb{R}. \quad (3)$$

and $\alpha \in \mathbb{R}$. We tested a range of values of α , and the kin verification accuracy was robust to its choice. Hence, $\alpha = 1$ was used.

3.1 Face Embedding

The backbone of the face embedding CNN is based on the Sphreface CNN [34], which was used by Robinson et al. [17] to achieve state-of-the-art kin-verification results. It is detailed in Table 1 where the embedding of an input image φ is given by the output of the FC-1 layer $\hat{\varphi} \in \mathbb{R}^{512}$. The output of FC-2 is used to refine the face embedding CNN using the RFIW dataset [17] and is optimized by the SphereLoss [34]. Each training sample consists of a pair $\{\phi_i, \varphi_i\}$ of input images, and both CNNs are jointly trained via weight sharing.

TABLE 1

The face embedding network. The CNN is based on the Sphreface CNN [34]. Residual units are shown in double-column brackets, and S2 denotes stride 2. The output of FC-1 is used as the embedding $\hat{\varphi}$ of the input image φ . The output of the layer FC-2 is used to refine the face embedding CNN.

Layer	20-layer Sphreface CNN
Conv1.x	$\begin{bmatrix} 3 \times 3, 64 \\ 3 \times 3, 64 \\ 3 \times 3, 64 \end{bmatrix} \times 1, S2$ $\times 1$
Conv2.x	$\begin{bmatrix} 3 \times 3, 128 \\ 3 \times 3, 128 \end{bmatrix} \times 1, S2$ $\times 2$
Conv3.x	$\begin{bmatrix} 3 \times 3, 256 \\ 3 \times 3, 256 \\ 3 \times 3, 256 \end{bmatrix} \times 1, S2$ $\times 4$
Conv4.x	$\begin{bmatrix} 3 \times 3, 512 \\ 3 \times 3, 512 \\ 3 \times 3, 512 \end{bmatrix} \times 1, S2$ $\times 1$
FC-1	512
FC-2	10, 676
SM	10, 676
Sphere loss	10, 676

3.2 The Fusion of Face Embeddings

The face embeddings $\{\hat{\varphi}_i, \hat{\phi}_i\} \in \mathbb{R}^{512}$ are fused to compute the kin verification scores. For that, we propose a novel

fusion subnetwork, whose core attribute is avoiding overfit that is common in kin verification CNNs due to the small training sets, and significant intraclass variability. An overview of the proposed fusion subnetwork is shown in Fig. 3. Concatenation and bilinear pooling [35] are com-

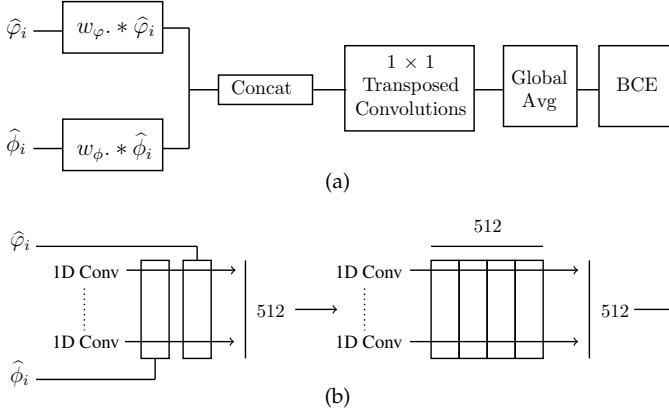


Fig. 3. The kinship classification subnetwork. Multiple such subnetworks are applied, one per kinship class. (a) The face embeddings $\hat{\varphi}_i$ and $\hat{\phi}_i$, are pointwise weighted (\cdot .) by the learnt weights w_φ and w_ϕ , respectively. The weighted embeddings are processed by the fusion subnetwork in Table 2. Average pooling and a Softmax activation are applied to the fused embedding, before the BCE loss. (b) The input layers of the proposed embedding fusion subnetwork. The embeddings $\hat{\varphi}_i \in \mathbb{R}^{512}$ and $\hat{\phi}_i \in \mathbb{R}^{512}$ are concatenated channel-wise, resulting in a $\mathbf{w} \in \mathbb{R}^{512 \times 2}$ activation map, that is processed by 512 1×1 transposed (channel-wise) convolutions, resulting in an $\mathbb{R}^{512 \times 512}$ activation.

mon embedding fusion approaches that are followed by corresponding FC layers. This requires a significant number of training parameters, resulting in overfitting, as exemplified in Section 4.3. Hence, we propose a novel low-capacity fusion subnetwork, that utilizes significantly fewer parameters. It is shown to provide better generalization and improves the verification accuracy. The core of the proposed fusion approach is depicted in Fig. 3b, where the inputs $\{\hat{\varphi}_i, \hat{\phi}_i\} \in \mathbb{R}^{512}$ are concatenated and processed *channel-wise*, such that the concatenated embedding is $\mathbf{w} \in \mathbb{R}^{512 \times 2}$. 1×1 channel-wise convolutions are then applied to \mathbf{w} and the succeeding activations maps as detailed in Table 2, such that their initial dimensionality ($d = 512$) is retained. As both embeddings $\{\hat{\varphi}_i, \hat{\phi}_i\}$ are computed by the same weight-sharing siamese CNN, and are the output of an FC layer, the corresponding entries in $\hat{\varphi}_i$ and $\hat{\phi}_i$ encode the same *semantic* content. The spatial locality in such embeddings is uninformative, implying that they can be processed by either an FC layer or 1×1 convolutions, as in the proposed scheme.

The face embeddings $\{\hat{\varphi}_i, \hat{\phi}_i\}$ are normalized element-wise before applying the fusion scheme

$$\begin{aligned} \hat{\varphi}_i^n &= \hat{\varphi}_i \cdot \mathbf{w}_\varphi \\ \hat{\phi}_i^n &= \hat{\phi}_i \cdot \mathbf{w}_\phi \end{aligned} \quad (4)$$

where $(\cdot \cdot \cdot)$ denotes pointwise multiplication and $\mathbf{w}_\varphi, \mathbf{w}_\phi \in \mathbb{R}^{512}$. Some of the kinship classes are symmetric in terms of gender (i.e. B-B, S-S, F-S, M-D), while others are asymmetric (F-D, M-S, SIBS). We utilize Eq. 4 to induce asymmetry in the kin verification CNN for the asymmetric

classes, by learning symmetric weights $\mathbf{w}_\varphi = \mathbf{w}_\phi = \mathbf{w}$ for the same-gender classes, and asymmetric weights $\mathbf{w}_\varphi, \mathbf{w}_\phi$ for the asymmetric ones.

TABLE 2

The proposed embedding fusion subnetwork. The input embeddings $\hat{\varphi}_i$ and $\hat{\phi}_i$, are channel-wise concatenated. A cascade of 1×1 convolutions is applied along the channels axis. Layers 1D Conv1-1D Conv8 are identical.

Layer	Kernel	Input	Activation	Output
Input		512×2		512×512
1D Conv1				
\vdots	1×1	512×512	Relu	512×512
1D Conv8				
1D Conv9	1×1	$512 \times 1,024$	Relu	512×1

3.3 Adaptive Sampling of Imbalanced Training Sets

Kinship verification datasets are inherently imbalanced with respect to multiple attributes. First, families differ significantly by the numbers of their images and the images per kin [17]. Second, following Table 3, the training pairs of some of the classes, such as F-S, F-D, M-S, and M-D are imbalanced, as most parents (M/F) in the RFIW dataset have multiple siblings (S/D), and will thus appear in notably more training pairs than any particular sibling. Thus, uniform sampling of the training pairs results in over-sampling of the parent classes (M/F), and families having more images than others. Due to the significant imbalances in the RFIW dataset [17], applying undersampling or over-sampling is impractical. Downsampling might result in a notably smaller training set, where kin verification training sets are relatively small to begin with. In contrast, oversampling might result in overfitting the smaller, oversampled sets. Let $f_k, k = 1..K$ be the families in the training set, and let $|f_k|$ be the number of image pairs of the k 'th family. We propose an adaptive sampling scheme, consisting of two steps, where we first set the *maximal* number of image pairs to be sampled from each family $|f_k|_{med} = median(|f_k|)$. For families where $|f_k| < |f_k|_{med}$, we only sample $|f_k|$ training pairs. To maximize the diversity of the training set, we choose the training images in the F-D, F-S, M-D, M-S kinship classes using cyclic buffers, one per family member (F, M, S, D). Thus, for each training pair, a different pair of images is chosen.

4 EXPERIMENTAL RESULTS

The proposed scheme was experimentally evaluated using the RFIW (Families In the Wild) dataset [17], that was found by Lopez et al. [15] and Damson et al. [16] to be the only unbiased kin verification dataset. The RFIW is the largest kin verification dataset depicting 1,000 different families, for a total of 11,932 images. There are 654,304 positive and negative pairs overall, and the images contain gender metadata. We followed the evaluation protocols detailed in [17], by applying the *restricted* protocol where the identities of the subjects in the dataset are unknown, and we are given predefined pairs of training images, per kinship class. Thus,

TABLE 3
The RFIW dataset [17]. The number of training and testing kin pairs per kinship class vary significantly.

Kinship	Train	Validation	Test
Brothers	29,812	55,546	18,196
Sisters	19,778	35,024	4,796
Siblings	28,428	15,422	9,716
Father-Daughter	41,604	35,238	15,040
Father-Son	64,826	44,870	18,166
Mother-Daughter	39,110	29,012	14,394
Mother-Son	66,464	31,094	14,806
Grfather-Grdaughter	1,478	4,846	838
Grfather-Grson	1,388	1,926	1,588
Grmother-Grdaughter	1,580	3,768	952
Grmother-Grson	1,284	1,844	1,470
Total	295,752	258,590	99,962

the adaptive sampling (Section 3.3), and the embedding fine-tuning can’t be applied. In the *unrestricted* protocol, both the identities and the kinship classes (F, M, B, S, etc.) are given, allowing to train using a significantly larger set of pairs.

Following Robinson et al. [17], we used a pre-trained VGG-Face face embedding [36] CNN, to compare with previous schemes based on that backbone. The fusion embedding subnetwork follows Section 3.2. In the *unrestricted* protocol, we used all of the CNN components detailed in Section 3, and the Spherefacer was finetuned using the RFIW dataset. The five-fold cross-validation split, as in [17], was used, with no family-overlap between the different folds. Negative pairs were sampled randomly, the same number as the positive ones.

4.1 Network Parameters and Training

The proposed approach was trained in two steps, where only the first step was applied in the *unrestricted* protocol. First, the face embedding CNN was trained using the CASIA-WebFace image dataset [33]. A SphereLoss was attached to the output of the layer FC-1 and applied using $l \in [5, 1500]$. The learning rate was gradually reduced from 0.01 to 0.0001 in 30 epochs, using an SGD optimizer.

In the second training step, applied for the *unrestricted* protocol, the RFIW dataset was used to jointly train a refined face embedding and a multi-task kin verification classifier. For that, the complete CNN, as depicted in Fig. 2, was used. Two SphereLosses were connected to the outputs of the FC-2 layer, for additional face embedding refinement, by classifying the faces in the RFIW dataset [17], and the multi-task kin verification subnetworks were jointly trained.

The MTCNN [37] was used to detect and align the faces in the training and test images. The face images were scaled to 108×108 pixels and augmented by changing the image gamma factor, scalings $s \in [0.5, 1, 2]$, horizontal flipping, and random jitter of $dx, dy \in [-2, 2]$. All of the augmentations were applied jointly and randomly. The weighting in Eq. 4 is applied differently to the symmetric (B-B, F-S, M-D, S-S) and asymmetric (F-D, M-S, SIBS) pairs of kins. The training pairs of the symmetric classes are randomly input to either the left or right side of the CNN. In contrast, each kin in the asymmetric classes is input to a predefined side of the CNN. We trained the network using the SGD optimizer

with a learning rate $\in [10^{-3}, 10^{-5}]$ for 30 epochs, where the learning rate was reduced by a factor of 10 when the loss decay flattened.

4.2 Kin Verification Results Using the RFIW Dataset

The proposed scheme was evaluated by applying it to the RFIW Dataset using both the *restricted* and *unrestricted* test protocols. We present the results of the FG2018 challenge [38] using the *restricted* protocol in Table 4. Our method is shown to be the most accurate, outperforming the second-best by 13.8%. In the *unrestricted* case, we compare to contemporary state-of-the-art results of the FG2018 [38] challenge. The *unrestricted* test protocol is more suitable for training deep CNNs, such as ours, as it provides a larger training set.

The FG2018 results are shown in Table 5. In the upper part of the table, we compare with kin verification schemes based on the VGG-Face [36] backbone. We cite the results of methods in which distance learning was applied on top of the VGG-Face backbone, that were implemented by Robinson et al. [17]. Our approach was also implemented using the VGG-Face backbone to allow fair comparison, and outperforms *all* previous methods, in *all* categories, but for the B-B class. Compared to the mDML scheme [43] having the second-highest average accuracy among all methods, we achieve an average accuracy improvement of 2.59%.

In the mid-segment of Table 5 (“Face embedding”), we compare with methods based on face embedding CNNs. Compared to the Spherefacer CNN [17], our approach shows an average improvement of 8.34%, exemplifying the upside of the proposed embedding fusion and classification subnetwork. Average improvements of 10.88% and 6.39% are achieved for the cross and intra-generation classes, respectively. Our approach is thus more accurate in verifying the more difficult cross-generation classes. Comparing our scheme implemented using the VGG-Face [36], to those based on the Spherefacer CNN [17] backbones, it follows that the Spherefacer-based ones are the more accurate. Last, we compared with recent state-of-the-art results [12], [27], that similar to our method, utilize both face embedding and metric learning. While these schemes outperform all of the “Face embedding” methods, they are outperformed by our approach in all categories.

The results for the FG2020 challenge [19] are reported in Table 6 and compared with the leading entries submitted to the FG2020 challenge, as reported on the challenge website. We could not apply our approach to the GFGD, GFGS, GMGD, and GMGS¹ categories, whose training sets are smaller by an order of magnitude (Table 3). It follows that our scheme outperforms all previous results on average, and in five out of eight kinship categories.

Qualitative kin verification examples of images from the RFIW dataset are depicted in Fig. 4. The reference images were chosen randomly and depict the common results. For the S-S and B-B kinship classes, the face similarity might seem intuitive. But the similarity of other kinship classes such as F-S, F-D, etc., seems to be unintuitive. In particular, comparing the True Positives with the False Positives

1. GF: grandfather, GM: grandmother, GD: granddaughter, GS: grandson.

TABLE 4

Kin verification results of the FG2018 challenge [38] using the *restricted* protocol. The results are given by of the accuracy percentage.

	M-D	M-S	S-S	B-B	SIBS	GM-GD	GM-GS	F-S	GF-GS	F-D	GF-GD	Avg.
#1	66.6	59.84	72.9	66.2	63.0	57.6	61.1	61.5	56.92	63.3	58.0	62.4
#2	65.8	60.46	70.2	68.4	61.6	57.0	62.8	61.2	56.4	63.1	59.42	62.4
#3	59.5	57.81	64.7	57.2	57.4	55.4	57.7	57.4	55.7	59.4	55.9	58.0
#4	61.5	60.5	68.0	62.7	59.0	54.5	52.2	58.6	53.3	58.21	57.9	58.7
#5	56.7	54.1	60.2	51.3	55.4	52.4	50.2	54.1	52.5	55.9	55.1	54.4
ours	73.8	70.9	77.3	69.1	68.6	63.9	63.3	68.9	63.7	68.9	61.9	68.2

TABLE 5

Kinship verification accuracy percentage using the RFIW dataset for methods applied to the *restricted* and *unrestricted* protocols.

Method	B-B	S-S	SIBS	F-D	F-S	M-D	M-S	Avg.
Handcrafted features								
LBP	55.5	57.5	55.4	55.1	53.8	55.7	54.7	55.4
SIFT	57.9	59.3	56.9	56.4	56.2	55.1	56.5	56.9
VGG-Face backbone								
+ITML	57.2	61.6	57.9	58.1	54.8	57.3	59.1	57.8
+LPP	67.6	66.2	71.0	62.5	61.4	65.04	63.5	65.3
+LMNN	67.1	68.3	66.99	65.7	67.1	68.1	66.2	67.0
+GmDAE	68.1	68.6	67.3	66.5	68.3	68.2	66.7	67.7
+DLML	68.0	68.9	68.0	66.0	68.00	68.5	67.2	67.8
+mDML	69.1	70.2	68.1	67.9	66.2	70.4	67.4	68.5
Ours (VGG)	69.1	77.3	68.6	68.9	68.9	73.8	70.9	71.1
Face embedding								
ResNet-22 [39]	66.6	69.7	60.1	59.5	60.3	61.5	59.4	62.3
VGG-Face [36]	69.7	75.4	66.5	64.3	63.9	66.4	62.8	66.7
ResNet+CF [40]	69.9	69.5	69.5	68.2	67.7	71.1	68.6	69.2
AdvNet [41]	71.8	77.4	69.8	67.8	68.8	69.9	67.3	70.4
VGG+Tri [42]	73.0	72.5	74.4	69.4	68.2	68.4	69.4	70.7
SphereFace [34]	71.9	77.3	70.2	69.3	68.5	71.8	69.5	71.2
Face Embedding + Learning								
ResNet+SDM [12]	72.6	79.4	70.4	68.3	68.0	71.3	68.8	71.2
KinNet [27]	84.2	81.7	72.7	72.8	77.3	75.8	76.3	77.2
Ours	85.9	86.3	78.0	77.4	74.9	76.9	75.6	79.6

TABLE 6

Kin verification results of the FG2020 challenge [19] using the *unrestricted* setup. The results are given by the accuracy percentage. We compare with the leading results submitted to the challenge.

	M-D	M-S	S-S	B-B	SIBS	F-S	F-D	S-S	Avg.
#1	0.78	0.74	0.8	0.8	0.77	0.81	0.75	0.8	0.77
#2	0.75	0.74	0.77	0.77	0.75	0.81	0.74	0.77	0.76
#3	0.75	0.75	0.74	0.75	0.72	0.82	0.76	0.74	0.75
#4	0.75	0.75	0.74	0.75	0.71	0.81	0.76	0.74	0.75
#5	0.74	0.75	0.74	0.75	0.72	0.81	0.75	0.74	0.75
ours	0.75	0.75	0.84	0.89	0.80	0.75	0.73	0.83	0.78

classifications does not provide insights, in contrast to face verification results.

4.3 Ablation Study

We conducted an ablation study reported in Table 8, wherein each experiment, we modified a single algorithmic component. Our approach was applied following the *unrestricted* protocol using the RFIW dataset, as in Section 4.2.

Adaptive sampling. We first studied the adaptive sampling scheme presented in Section 3.3. The statistics of the RFIW dataset [17], with and without applying the adaptive sampling, are reported in Table 7 and exemplify the balancing effect. The variations in the mean and standard

deviation of the balanced RFIW are notably smaller. To compare the corresponding kin verification accuracy, we trained a network following our approach, without the adaptive sampling. Instead, we used the common random sampling. The proposed adaptive sampling is shown to improve the classification accuracy by a significant 4.44%.

TABLE 7

The number of images per family and family member in the RFIW dataset [17], with and without applying the adaptive sampling introduced in Section 3.3. Using the adaptive sampling, the dataset's statistics are balanced.

Fold#	#Images per family			#Images per family member		
	Maximum	Mean	Std	Maximum	Mean	Std
RFIW						
1	1,312	111	160	656	34	56
2	1,532	114	204	722	36	66
3	760	97	136	380	30	43
4	15,132	265	1,571	2,688	76	297
5	6,808	190	699	2,373	57	169
Balanced RFIW						
1	1,600	125	224	387	37	52
2	1,600	121	213	540	36	54
3	1,600	118	199	380	36	51
4	1,532	116	193	722	35	60
5	1,312	112	174	656	35	59

Multi-task training. The multi-task training was evaluated by training a different CNN for each kinship class

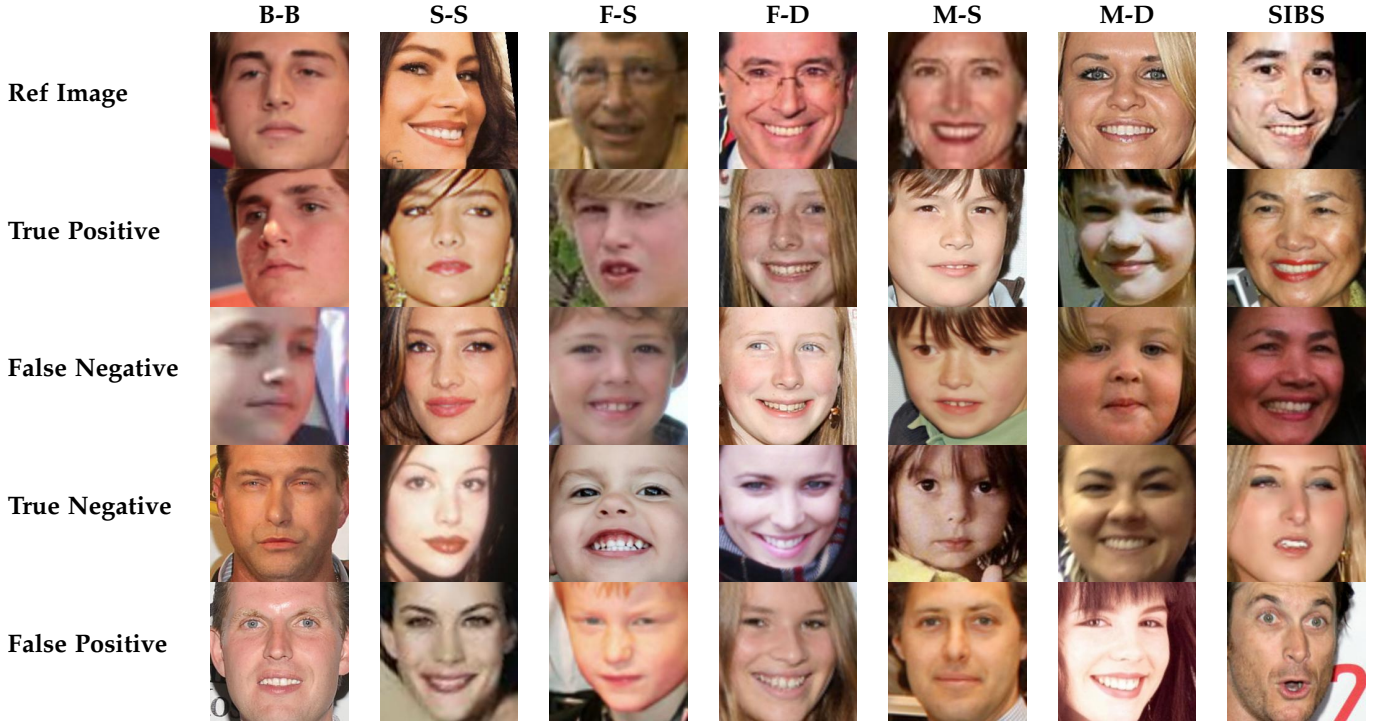


Fig. 4. Kin verification examples from the RFIW dataset [17], as classified by the proposed scheme. The upper row shows a face image, and the succeeding rows depict the corresponding kin verification results.

instead of the unified approach, as in Section 3. Each of the multiple single-task face-embedding CNNs was refined as in the first phase in Section 4.1. For that, we used the RFIW dataset and enabled one of the Sphere losses $L_{Sphere}^{\hat{\varphi}_i, \hat{\phi}}$ as in Fig. 2. The fusion and classification subnetworks were then trained separately per kinship class. The results show that the proposed multi-task training provides an average accuracy improvement of 1.1%, implying that different kinship classes share a joint structure utilized by the proposed scheme to improve accuracy.

Embedding-fusion scheme. The embedding-fusion subnetwork, introduced in Section 3.2, was studied by replacing it with the common fusion approach where the embeddings $\hat{\varphi}_i, \hat{\phi} \in \mathbb{R}^{512}$ were concatenated, followed by an FC layer. This results in a significant accuracy degradation of close to 25%, compared with our scheme. We attribute that to overfitting, as kin verification is characterized by significant intraclass variability. We also applied our approach without using a fusion scheme, such that the face embeddings were used for kin verification, as in [17]. In such a scheme, there is no overfit, but the results are inferior by 5.9%.

Asymmetric normalization. We studied the use of the asymmetric normalization in Eq. 4 by applying the proposed scheme without the normalization, and by using symmetric weights $w_\varphi = w_\phi$. Using the asymmetric weights improves the average accuracy by 0.65% and 0.57%, compared to not applying the weighting, and using symmetric weights, respectively.

5 CONCLUSIONS

In this work, we proposed a multi-task deep learning-based approach for kin verification, where all kinship classes are

jointly trained, utilizing all of the training data. We also introduced a novel embedding fusion scheme to fuse the face embeddings of the input subjects, that is shown to avoid the overfitting issues common in kin verification, and provides notable accuracy improvement. An adaptive sampling of the training pairs in the RFIW dataset allows creating a balanced training set that further improves the kin verification accuracy. Our scheme is experimentally shown to achieve state-of-the-art accuracy when applied to the RFIW, FG2018, and FG2020 datasets in both the *restricted* and *unrestricted* test protocols.

REFERENCES

- [1] Y. Wu, Z. Ding, H. Liu, J. Robinson, and Y. Fu, "Kinship classification through latent adaptive subspace," in *2018 IEEE International Conference on Automatic Face and Gesture Recognition*. IEEE, 2018, pp. 143–149.
- [2] R. Fang, A. Gallagher, T. Chen, and A. Loui, "Kinship classification by modeling facial feature heredity," in *Proc. Int. Conf. Image Process.*, 2013, pp. 2983–2987.
- [3] M. Xu and Y. Shang, "Kinship verification using facial images by robust similarity learning," in *Math. Problems Eng.* vol. 2016.
- [4] X. Zhou, Y. Shang, H. Yan, and G. Guo, "Ensemble similarity learning for kinship verification from facial images in the wild," *Information Fusion*, vol. 32, pp. 40–48, 2016.
- [5] R. Fang, K. D. Tang, N. Snavely, and T. Chen, "Towards computational models of kinship verification," in *IEEE International Conference on Image Processing*, 2010, pp. 1577–1580.
- [6] A. Puthenputhussery, Q. Liu, and C. Liu, "SIFT flow based genetic fisher vector feature for kinship verification," in *IEEE International Conference on Image Processing (ICIP)*, Sep. 2016, pp. 2921–2925.
- [7] A. R. Dandekar and M. S. Nimbarte, "Verification of family relation from parents and child facial images," in *International Conference on Power, Automation and Communication (INPAC)*, Oct 2014, pp. 157–162.

TABLE 8
Ablation study results. The results are given by of the accuracy percentage.

	B-B	S-S	SIBS	F-S	F-D	M-S	M-D	Average
Fusion by concatenation	57.18	55.01	53.71	57.97	54.23	55.72	55.74	55.65
Face embedding only	77.35	81.22	70.19	69.86	72.67	71.77	72.50	73.65
FIW random sampling	78.33	84.35	70.23	71.64	74.43	73.06	73.00	75.00
Single task training	84.99	84.96	74.63	75.07	74.64	76.74	77.96	78.42
No normalization	85.69	86.03	74.56	76.36	75.29	76.14	78.25	78.90
Symmetric normalization	85.77	86.14	74.50	77.25	75.34	75.87	78.05	78.98
Ours	85.89	86.26	74.86	77.39	75.59	76.89	79.98	79.55

- [8] L. Zheng, K. Idrissi, C. Garcia, S. Duffner, and A. Baskurt, "Triangular Similarity Metric Learning for Face Verification," in *IEEE International Conference on Automatic Face and Gesture Recognition (FG 2015)*, vol. 1, May 2015, pp. 1–7.
- [9] H. Yan, J. Lu, W. Deng, and X. Zhou, "Discriminative multimetric learning for kinship verification," *Information Forensics and Security, IEEE Transactions on*, vol. 9, no. 7, pp. 1169–1178, July 2014.
- [10] H. Yan, "Kinship verification using neighborhood repulsed correlation metric learning," *Image and Vision Computing*, vol. 60, pp. 91–97, 2017.
- [11] Q. Duan, L. Zhang, and W. Zuo, "From face recognition to kinship verification: An adaptation approach," in *IEEE International Conference on Computer Vision Workshops (ICCVW)*, Oct 2017, pp. 1590–1598.
- [12] S. Wang, Z. Ding, and Y. Fu, "Cross-generation kinship verification with sparse discriminative metric," *IEEE Transactions on Pattern Analysis and Machine Intelligence*, vol. 41, no. 11, pp. 2783–2790, Nov 2019.
- [13] S. Xia, M. Shao, J. Luo, and Y. Fu, "Understanding kin relationships in a photo," *IEEE Transactions on Multimedia*, vol. 14, no. 4, pp. 1046–1056, Aug 2012.
- [14] J. Lu et al., "The FG 2015 kinship verification in the wild evaluation," in *IEEE International Conference and Workshops on Automatic Face and Gesture Recognition (FG)*, vol. 1, 2015, pp. 1–7.
- [15] M. B. Lpez, E. Boutellaa, and A. Hadid, "Comments on the kinship face in the wild data sets," *IEEE Transactions on Pattern Analysis and Machine Intelligence*, vol. 38, no. 11, pp. 2342–2344, Nov 2016.
- [16] M. Dawson, A. Zisserman, and C. Nellaker, "From same photo: Cheating on visual kinship challenges," *Lecture Notes in Computer Science*, pp. 654–668, 2019.
- [17] J. P. Robinson, M. Shao, Y. Wu, H. Liu, T. Gillis, and Y. Fu, "Visual kinship recognition of families in the wild," *IEEE Transactions on Pattern Analysis and Machine Intelligence*, vol. 40, no. 11, pp. 2624–2637, Nov 2018.
- [18] J. P. Robinson, Z. Khan, Y. Yin, M. Shao, and Y. Fu, "Families in wild multimedia (fiw-mm): A multi-modal database for recognizing kinship," *ArXiv*, vol. abs/2007.14509, 2020.
- [19] J. P. Robinson, Y. Yin, Z. Khan, M. Shao, S. Xia, M. Stopa, S. Timoner, M. A. Turk, R. Chellappa, and Y. Fu, "Recognizing families in the wild (RFIW): The 4th edition," 2020.
- [20] X. Qin, X. Tan, and S. Chen, "Tri-subject kinship verification: Understanding the core of a family," *IEEE Transactions on Multimedia*, vol. 17, no. 10, pp. 1855–1867, Oct 2015.
- [21] S. Mahpod and Y. Keller, "Kinship verification using multiview hybrid distance learning," *Computer Vision and Image Understanding*, vol. 167, pp. 28–36, 2018.
- [22] E. Dahan, Y. Keller, and S. Mahpod, "Kin-verification model on fiw dataset using multi-set learning and local features," in *RFIW '17: Proceedings of the 2017 Workshop on Recognizing Families In the Wild*, October 2017, pp. 31–35.
- [23] M. Xu and Y. Shang, "Kinship measurement on face images by structured similarity fusion," *IEEE Access*, vol. 4, pp. 10 280–10 287, 2016.
- [24] J. Lu, J. Hu, and Y. Tan, "Discriminative deep metric learning for face and kinship verification," *IEEE Transactions on Image Processing*, vol. 26, no. 9, pp. 4269–4282, Sep. 2017.
- [25] A. Mignon and F. Jurie, "CMMML: a New Metric Learning Approach for Cross Modal Matching," in *Asian Conference on Computer Vision*, South Korea, Nov. 2012.
- [26] N. Kohli, M. Vatsa, R. Singh, A. Noore, and A. Majumdar, "Hierarchical representation learning for kinship verification," *IEEE Transactions on Image Processing*, vol. 26, no. 1, pp. 289–302, Jan 2017.
- [27] Y. Li, J. Zeng, J. Zhang, A. Dai, M. Kan, S. Shan, and X. Chen, "KinNet: Fine-to-coarse deep metric learning for kinship verification," in *Proceedings of the 2017 Workshop on Recognizing Families In the Wild*, ser. RFIW 17, New York, NY, USA, 2017, p. 1320.
- [28] N. Kohli, D. Yadav, M. Vatsa, R. Singh, and A. Noore, "Supervised mixed norm autoencoder for kinship verification in unconstrained videos," *IEEE Transactions on Image Processing*, vol. 28, no. 3, pp. 1329–1341, 2019.
- [29] S. Wang, Z. Ding, and Y. Fu, "Coupled marginalized auto-encoders for cross-domain multi-view learning," in *Proceedings of the International Joint Conference on Artificial Intelligence*, ser. IJCAI'16. AAAI Press, 2016, pp. 2125–2131.
- [30] S. Ozkan and A. Ozkan, "KinshipGAN: Synthesizing of kinship faces from family photos by regularizing a deep face network," in *2018 25th IEEE International Conference on Image Processing (ICIP)*, 2018, pp. 2142–2146.
- [31] P. Gao, S. Xia, J. Robinson, J. Zhang, C. Xia, M. Shao, and Y. Fu, "What will your child look like? DNA-Net: Age and gender aware kin face synthesizer," *arXiv e-prints*, p. arXiv:1911.07014, Nov 2019.
- [32] J. P. Robinson, M. Shao, and Y. Fu, "Visual kinship recognition: A decade in the making," *ArXiv*, vol. abs/2006.16033, 2020.
- [33] D. Yi, Z. Lei, S. Liao, and S. Z. Li, "Learning Face Representation from Scratch," *arXiv e-prints*, p. arXiv:1411.7923, Nov 2014.
- [34] W. Liu, Y. Wen, Z. Yu, M. Li, B. Raj, and L. Song, "Sphereface: Deep hypersphere embedding for face recognition," *2017 IEEE Conference on Computer Vision and Pattern Recognition (CVPR)*, pp. 6738–6746, Jul 2017.
- [35] T. Lin, A. RoyChowdhury, and S. Maji, "Bilinear CNN models for fine-grained visual recognition," in *2015 IEEE International Conference on Computer Vision (ICCV)*, 2015, pp. 1449–1457.
- [36] O. M. Parkhi, A. Vedaldi, A. Zisserman et al., "Deep face recognition," in *British Machine Vision Conference*, vol. 1, no. 3, 2015, p. 6.
- [37] K. Zhang, Z. Zhang, Z. Li, and Y. Qiao, "Joint face detection and alignment using multitask cascaded convolutional networks," *IEEE Signal Processing Letters*, vol. 23, no. 10, pp. 1499–1503, Oct 2016.
- [38] J. P. Robinson, M. Shao, Y. Wu, H. Liu, T. Gillis, and Y. Fu, "Visual kinship recognition of families in the wild," 2018.
- [39] Y. Wen, K. Zhang, Z. Li, and Y. Qiao, "A discriminative feature learning approach for deep face recognition," in *Proceedings of the European Conference on Computer Vision (ECCV)*, vol. 9911, 2016, pp. 499–515.
- [40] J. P. Robinson, M. Shao, H. Zhao, Y. Wu, T. Gillis, and Y. Fu, "Recognizing families in the wild (RFIW): Data challenge workshop in conjunction with acm mm 2017," in *Proceedings of the 2017 Workshop on Recognizing Families In the Wild*, ser. RFIW 17, New York, NY, USA, 2017, p. 512.
- [41] Q. Duan and L. Zhang, "Advnet: Adversarial contrastive residual net for 1 million kinship recognition," in *Proceedings of the 2017 Workshop on Recognizing Families In the Wild*. ACM, 2017, pp. 21–29.
- [42] J. P. Robinson, M. Shao, Y. Wu, and Y. Fu, "Families in the wild (FIW): Large-scale kinship image database and benchmarks," in *Proceedings of the 24th ACM international conference on Multimedia*. ACM, 2016, pp. 242–246.
- [43] S. Wang, J. P. Robinson, and Y. Fu, "Kinship verification on families in the wild with marginalized denoising metric learning," in *IEEE International Conference on Automatic Face Gesture Recognition (FG 2017)*, 2017, pp. 216–221.